# Guided Self-Assembly of Symmetric Diblock Copolymer Films on Chemically Nanopatterned Substrates

**Xiao M. Yang, Richard D. Peters, and Paul F. Nealey***

*Department of Chemical Engineering and Center for Nanotechnology, University of Wisconsin, Madison, Wisconsin 53706*

**Harun H. Solak and Franco Cerrina**

*Department of Electrical and Computer Engineering and Center for Nanotechnology, University of Wisconsin, Madison, Wisconsin 53706*

*Received July 27, 2000; Revised Manuscript Received October 26, 2000*

ABSTRACT: Self-assembled films of octadecyltrichlorosilane were patterned with regions of different chemical functionality using extreme ultraviolet interferometric lithography. Unexposed regions of the imaging layers remain terminated in methyl groups, and exposed regions are modified so as to be terminated with polar, oxygen-containing terminal groups. Thin films of symmetric poly(styrene-*b*-methyl methacrylate) were deposited on the substrates and annealed. Unexposed and exposed regions are preferentially wet by the polystyrene block and poly(methyl methacrylate) block of the copolymer, respectively. The dimensions of the grating patterns on the substrate had periods ($L_s$) from 1400 to ~60 nm. If $L_s \gg L_o$ ($L_o$ = bulk lamellar period of the block copolymer), then the surface pattern was replicated in the topography of the polymer film with a maximum difference in film thickness of $^1/_2L_o$ on adjacent regions. The topographic pattern of the polymer film was a result of lamellae oriented parallel to the substrate with symmetric wetting on unexposed regions (thickness = $nL_o$) and with asymmetric wetting on exposed regions (thickness = $(n + ^1/_2)L_o$). As the dimension of $L_s$ approached $L_o$, the replication of the surface pattern in the topography of the film continued to be observed, but with decreasing difference in thickness over adjacent exposed and unexposed regions. For a surface pattern with $L_s \approx L_o$, the lamellae oriented perpendicular to the substrate and were macroscopically aligned with the surface pattern.

## Introduction

The use of block copolymer thin films as templates for patterning has great potential for applications in nanotechnology.[1,2] Block copolymers self-assemble into periodic structures with length scales of 10−100 nm in the bulk.[3,4] The size and the shape of the microphase-separated domains can be controlled by the molecular weight and composition of the diblock copolymer. In patterning applications, thin films of block copolymers typically are employed. A common strategy is to use the microphase-separated domain structures as a template; following self-assembly one block of the copolymer is selectively removed, and the remaining patterned material serves as an etch mask for pattern transfer into the substrate.[2] Films can be prepared easily over large areas by current coating techniques. A formidable challenge is to control orientation and perfection of ordering[5] of the domains in the thin films over large areas.

Interfacial energies between the blocks of symmetric block copolymers and substrates in thin films govern the orientation of the microphase-separated domains such that the lamellae generally orient parallel to the plane of the film. In addition, the minimization of the total free energy of films with a free surface requires the thickness to be quantized in terms of $L_o$.[6−9] Several techniques have been demonstrated to align and orient domains in thin films of block copolymers. Morkved et al.[10a] and Mansky et al.[10b] used electric fields to align cylindrical domains of poly(styrene-*b*-methyl methacrylate) (P(S-*b*-MMA)) along the electric field lines in the plane of the film. Russell and co-workers used two

techniques to achieve perpendicular orientation of domains: (1) random copolymer brushes of neutral composition to induce perpendicular orientation of both lamellar domains and cylindrical domains in symmetric and asymmetric P(S-*b*-MMA), respectively,[11a−e] and (2) electric fields applied normal to the plane of a polymer film to orient cylindrical domains of P(S-*b*-MMA) perpendicular to the substrate.[11e,f] The cylinders were arranged in hexagonal arrays with perfection in the ordering over grain sizes similar to those observed in the bulk. Fasolka et al. cast ultrathin films of poly-(styrene-*b*-*n*-butyl methacrylate) on miscut silicon wafers and observed ordered morphologies along the corrugations of the substrate induced by thickness variations in the polymer film.[12] Rockford et al. obliquely deposited gold on miscut silicon wafers to produce alternating stripes of gold and silicon oxide with periods of 60 ± 10 nm.[13] Lamellar domains of symmetric P(S-*b*-MMA) oriented perpendicular to the substrate with greatest macroscopic ordering for patterns of gold and silicon oxide that were commensurate with the bulk lamellar period of the block copolymer. Gold was preferentially wet by polystyrene, and silicon oxide was preferentially wet by poly(methyl methacrylate). Recently, Segalman et al. reported the use of sidewall constraints to induce long-range ordering of spherical domains over regions with dimensions as large as 4−5 $\mu$m.[14] These experiments were particularly elegant in that the ordering was induced on chemically homogeneous substrates.

In this paper we demonstrate a technique to induce orientation of lamellar domains of a symmetric block copolymer film perpendicular to the surface, with per-

* Corresponding author: nealey@engr.wisc.edu.

fection in the ordering over macroscopic dimensions and with the ability to register or align the domains with features of the substrate. Our strategy combines advanced lithographic techniques and guided self-assembly of the block copolymer film. Organic imaging layers are patterned using an advanced lithographic tool, i.e., extreme ultraviolet interferometric lithography (EUV-IL). Regions of the imaging layer that are exposed to radiation undergo a chemical transformation that alters the surface chemistry of the imaging layer. A thin film of a symmetric diblock copolymer is deposited on the patterned imaging layer and annealed above the glass transition temperature of the blocks of the copolymer. During annealing, the lamellar domains of the copolymer film self-assemble such that adjacent regions of the chemically patterned surface are preferentially wet by the different blocks of the copolymer. The lamellae orient perpendicular to the plane of the film and amplify the surface pattern. The advanced lithographic step allows for registration and alignment and may ultimately allow the fabrication of addressable arrays from block copolymer templates.

Evidence that the strategy described above will be successful is derived from theoretical research in addition to the seminal experimental work of Rockford et al.[13] Wang et al. investigated the morphology of symmetric diblock copolymer films confined between a homogeneous surface and a striped patterned surface using Monte Carlo simulations.[15] With knowledge of the self-assembled structures that are observed for different combinations of pattern period and polymer interaction with the confining walls, Wang et al. rationalized the results of the molecular simulations and constructed phase diagrams using a phenomenological model.[16−19] This model and other theoretical formalisms had also been applied previously by others to predict the behavior of diblock copolymer films on chemically patterned surfaces.[20−25] From the theoretical investigations, the following optimal conditions were identified that lead to amplification of the surface pattern with self-assembled perpendicular lamellae throughout the thickness of the polymer film: (1) the period of the patterned surface, $L_s$, was nearly equal to $L_o$, and (2) the confining homogeneous surface of the film had neutral wetting conditions (equal affinity for both blocks of the copolymer). One important difference between the theoretical work and the experiments relates to the boundary conditions of the polymer films. In the theoretical research, the films are confined between hard walls, but in the experiments, one of the surfaces of the film is a free surface.

We have previously reported on a number of advancements to implement our strategy to guide the self-assembly of symmetric diblock copolymer films experimentally. Self-assembled (SA) films of octadecyltrichlorosilane (OTS) were investigated as organic imaging layers in conjunction with block copolymer films of P(S-*b*-MMA). The surface chemistry of OTS was modified by exposure to X-rays or EUV radiation in air such that the initial nonpolar, hydrophobic surface becomes polar and hydrophilic by the incorporation of hydroxyl and aldehyde terminal groups.[26] The wetting behavior of films of P(S-*b*-MMA) on exposed OTS was tuned such that the PS block preferentially wets unexposed OTS and the PMMA block preferentially wets exposed OTS.[27,28] In collaboration with Cerrina et al., we also invented an exposure tool capable of patterning at the

scale of tens of nanometers.[29,30] The tool is essentially a Lloyd's mirror interferometer designed for use with extreme ultraviolet radiation.

In this paper, we pattern chemical gratings on SA films of OTS using EUV-IL with periods from 1400 to 60 nm. The behavior of films of P(S-*b*-MMA) on these surfaces is studied as a function of the ratio of $L_s$ to $L_o$. For $L_s > L_o$, the surface patterns are transferred into the polymer film resulting in height variations on the surface. For $L_s = L_o$, the surface patterns are amplified by perpendicular lamellae. The two regimes of behavior are discussed in terms of the lamellar structure and orientation in the polymer films.

## Experimental Section

**Materials.** Polished 100 mm diameter silicon ⟨100⟩ wafers were purchased from Tygh Silicon and used as substrates for deposition of films. Octadecyltrichlorosilane (CH₃(CH₂)₁₇SiCl₃, 95%) was purchased from Gelest and was used as received. Toluene (99.8%, anhydrous), and chlorofrom (99+%, anhydrous) were purchased from Aldrich and were used without further purification. Symmetric poly(styrene-*block*-methyl methacrylate) block copolymers were purchased from Polymer Source Inc. Two molecular weights of P(S-*b*-MMA) were used in our experiments: (1) number-average molar mass = 51 200 g/mol, polydispersity = 1.06, styrene volume fraction = 0.48, and $L_o \sim 30$ nm; (2) number-average molar mass = 143 500 g/mol, polydispersity = 1.09, styrene volume fraction = 0.51, and $L_o \sim 66$ nm.

**Preparation and Characterization of SA Films of OTS.** The silicon wafers were cleaned by immersion in a piranha solution (7:3 (v:v) of 98% H₂SO₄/30% H₂O₂) at 90 °C for 30 min. The silicon wafers were immediately rinsed with deionized water (resistivity ≥ 18 MΩ/cm) several times and were blown dry with nitrogen. The cleansed substrates were immersed in a 0.1% (v/v) solution of OTS in toluene in a glovebox with a nitrogen atmosphere.[26] The typical immersion times used here ranged from 24 to 30 h. After the substrates were removed from the silane solution, they were rinsed with chloroform for approximately 30 s, and excess chloroform was allowed to evaporate. The films were rinsed with absolute ethanol and were dried under a stream of nitrogen. Advancing contact angles of deionized water on OTS were measured using a Ramé-Hart goniometer, and the typical value was about 105 ± 3°. Previously, we have shown that films of P(S-*b*-MMA) on the surface of SA films of OTS deposited under identical conditions exhibited symmetric wetting behavior after annealing at 180 °C for 24 h.[28]

**Patterning of SA Films of OTS by EUV Interferometric Lithography.** OTS was exposed to EUV radiation ($\lambda = 13.4$ nm) radiation using the EUV interferometer system at the Center for Nanotechnology in Madison, WI.[29,30] A description of the system is included in the Results and Discussion section. The exposures were carried out in a chamber with a pressure of 100 mTorr of oxygen. The intensity of the incident radiation to the surface of SA films was ~10 mW/cm². The period of the fringe pattern for all exposures was verified by patterning UV6 photoresist (Shipley) after the system was configured with a particular geometry.[29,30] Metrology of the photoresist was performed using scanning electron microscopy (Hitachi 6180 CD). The line and space structures of photoresist were often not exactly symmetric, as is the latent image (the interference pattern), but the period does not depend on symmetry and could be accurately determined by averaging over a large number of structures.

**Deposition of Diblock Copolymer on Patterned OTS.** Thin films of P(S-*b*-MMA) were deposited onto patterned OTS substrates by spin-coating from dilute solutions (2% w/w) of the copolymers in toluene. Films were spun at rates from 2500 to 3000 rpm for 60 s. The initial thicknesses of the films were determined using a Rudolf Research/Auto EL II ellipsometer using a He−Ne laser ($\lambda = 632.8$ nm) at an incident angle of 70° relative to the surface normal of the substrates. The use
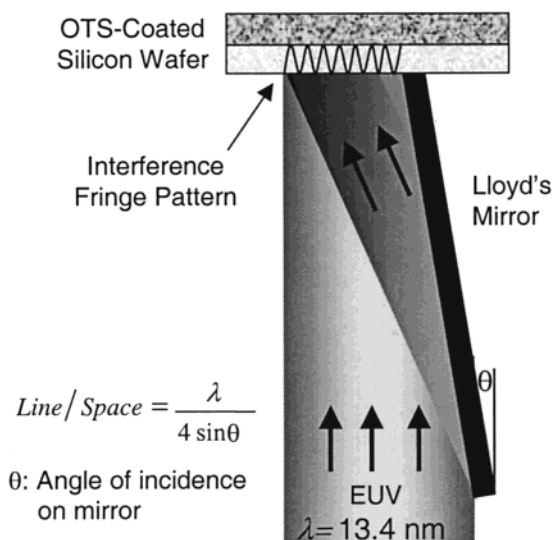
**Figure 1.** Schematic of the Lloyd's mirror interferometer exposure system on the EUV beamline. The reflected beam from the mirror interferes with the direct beam at the substrate to produce the interference pattern. The fringe period is given by $\lambda/(2 \sin \theta)$ where $\theta$ is the angle of incidence with the mirror.

of the ellipsometer to measure the thicknesses of the P(S-*b*-MMA) films required an assumption about the index of refraction, $n$, for the microphase-separated material. We assumed $n$ was the same as for polystyrene, and the results were consistent with measurements using a profilometer. The polymer films were annealed at 180 °C in a vacuum oven for 24 h. After annealing, the films were investigated using atomic force microscopy (AFM) and transmission electron microscopy (TEM).

**Atomic Force Microscopy.** The surface topography of the polymer films was characterized using AFM. AFM measurements were performed in air in both contact mode and tapping mode with a Nanoscope III MultiMode system (Digital Instruments). In tapping mode, both topography and phase image were obtained simultaneously. The typical imaging force in contact mode was on the order of $10^{-9}$ N. We used both oxide-sharpened silicon nitride tips (radii = 5–40 nm, Digital Instruments) and carbon nanotips (radii < 5 nm, Piezomax Technologies, Inc.) to image the topography of the polymer surface.

**Transmission Electron Microscopy.** The internal structure of the films was studied using TEM. TEM was performed on a JEOL 200CX at 200 kV in the bright field mode at the Materials Science Center at the University of Wisconsin–Madison. Samples were imaged in plane-view. A layer of carbon (ca. 20 nm thick) was evaporated onto the surface of films and then covered with a 25% aqueous solution of poly-(acrylic acid) (PAA). After the sample was dried in air overnight, the P(S-*b*-MMA)–carbon–PAA composite was peeled off the substrate and floated on deionized water with the PAA side down. After the PAA layer dissolved, the floating film was collected onto TEM grids. The films were then exposed to the vapor of the RuO$_4$ solution for 15 min. The RuO$_4$ selectively stains the PS block and provides contrast in electron density.

## Results and Discussion

A schematic of the EUV interferometer exposure system is presented in Figure 1.[29,30] An Au-coated polished silicon wafer (prepared by vacuum deposition with a root-mean-square roughness < 0.32 nm) was used as a Lloyd's mirror to reflect part of an incident beam at grazing incidence and interfere with the direct beam at the sample plane. The fringe period is given by $\lambda/(2 \sin \theta)$ where $\theta$ is the angle of incidence with the Lloyd's mirror. The theoretical limit is 6.7 nm for the

minimum printable period for incident radiation with a wavelength of 13.4 nm. An OTS-covered silicon wafer is placed at the downstream end of the mirror so as to irradiate the sample with the interference fringe patterns. The number of fringes depends on the spatial and temporal coherence of the source. The spatial coherence depends on the size of the light source and distance from the source. In our experimental setup, temporal coherence ultimately limits the number of fringes, and the source can be considered to be spatially coherent for practical purposes.[30] The finite temporal coherence limits the allowed optical path difference between the direct and reflected beams for producing fringes. The number of fringes, $m$, is proportional to $\lambda/\Delta\lambda$.[29] The interferometer can be operated with or without a monochromator in the path of the beam before the mirror. With the monochromator, the beam intensity is low, but $\lambda/\Delta\lambda$ is approximately 1000. In this mode, approximately 1000 fringes were produced. If the fringe period was 40 nm, for example, the width of the patterned area observed in patterns of photoresist was 40 $\mu$m. Without the monochromator, the number of the fringes produced is 15–20 ($\lambda/\Delta\lambda \approx 15$–20), but the intensity of the beam is approximately 60 times greater than that of the monochromatic beam. Because of differences in sensitivity and contrast between photoresist and OTS imaging layer, the number of fringes that were observed in patterned photoresist was significantly greater than the number of fringes that were observed on patterned OTS. Exposures of OTS with grating periods of ~60 nm were performed without the monochromator so as to reduce the exposure times to approximately 50–60 s compared to ~1 h with the monochromator. The length of the exposed area corresponded to the width of the beam, ~5 mm. The 30 nm features on the patterned SA films of OTS with the smallest grating periods are the smallest reported features on SA films of alkylsiloxanes patterned using a parallel patterning technique.

Figure 2 shows an AFM image of the surface of a P(S-*b*-MMA) film after it was deposited and annealed on OTS that had been exposed in the EUV interferometer. The period of the fringe pattern, $L_s$, was 900 nm. The initial film thickness of the block copolymer was 66 ± 2 nm ($2.2L_o$). With knowledge of the initial film thickness and $L_o$, the formation of topography on the surface of the film and the type of topography were used to determine the wetting of the block copolymer at the substrate. For the initial thickness of $2.2L_o$, island formation was indicative of symmetric wetting, and hole formation was indicative of asymmetric wetting. Three different regions were observed on this sample. The left side of the surface was unexposed because it was in the shadow of the mirror. Islands with heights of ~30 nm ($L_o$) were observed in this region, indicating symmetric wetting of the block copolymer with the PS block at the polymer–substrate interface and at the free surface. The right side of the surface was uniformly exposed because this region is outside the area where coherent fringes are produced. Holes with depths of ~30 nm were observed in the exposed region, indicating asymmetric wetting of the block copolymer. In this case, the PMMA block preferentially wet the polymer–substrate interface, and PS was present at the free surface. On the patterned region in the middle, the topography of the block copolymer film replicated the period of the fringes of the EUV exposure. AFM measurements showed that
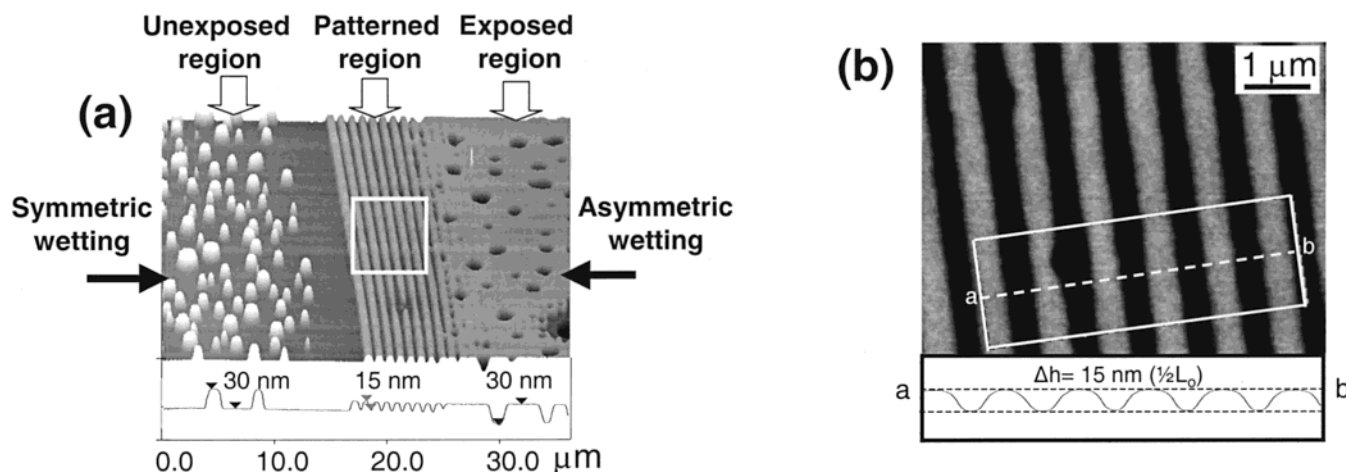
**Figure 2.** (a) AFM image of the surface of a P(S-*b*-MMA) ($L_o$ = 30 nm) film after deposition and annealing on a chemically patterned surface with a period of 900 nm. The initial film thickness was ~$2.2L_o$ (66 ± 2 nm). Unexposed regions showed island topography with a height of ~30 nm ($L_o$), indicating symmetric wetting. The topography of the P(S-*b*-MMA) film on patterned regions replicated the underlying pattern of the OTS due to different wetting behavior on adjacent stripes. Exposed regions showed hole topography with a depth of ~30 nm ($L_o$), indicating asymmetric wetting. (b) AFM image of the topography of the film on the patterned region marked in Figure 1a. The difference in height between adjacent regions was ~15 nm ($^1/_2L_o$).

the pattern period was 900 nm, and the difference in height between adjacent regions was 15 nm.

We interpret these results based on our previous reports detailing the chemical modification of OTS upon exposure to X-rays ($\lambda \approx$ 1 nm, $\Delta \lambda/\lambda \approx$ 3)[26] and the wetting behavior of P(S-*b*-MMA) films on OTS and OTS exposed to X-rays in the presence of oxygen.[27,28] Exposure of OTS to X-rays results in the incorporation of oxygen-containing functional groups on the surface of the film. Primary and secondary electrons generated by the interaction of the X-rays with the substrate are primarily responsible for the photochemical reactions.[26,31,32] The chemical modification of OTS exposed to EUV radiation is expected to follow the same mechanism as that for X-ray exposures. The wetting behavior of P(S-*b*-MMA) films on OTS-covered substrates can be tuned from symmetric to neutral to asymmetric wetting with increasing dose of X-rays.[27] The transitions in wetting behavior were correlated to relative values of interfacial energy for the PS and PMMA blocks on these surfaces. The wetting behavior observed on OTS exposed to EUV radiation follows the same trends: symmetric wetting was observed on unexposed OTS[28] or OTS exposed to low doses,[27] and asymmetric wetting was observed on OTS exposed to high doses.[27] The topography observed in the middle regions is identical to that observed on OTS patterned with X-ray lithography with dimensions of 150–1000 nm.[33] Adjacent exposed and unexposed regions exhibited asymmetric and symmetric wetting, respectively, and the block copolymer film differed in height by 15 nm ($^1/_2L_o$) across adjacent regions. The height difference of $^1/_2L_o$ corresponded to the difference in quantized thickness between symmetric and asymmetric wetting behavior.[6–9]

Figure 3 shows two typical AFM images of the surface of P(S-*b*-MMA) films after they were annealed on OTS that had been patterned with EUV interferometer with periods of 240 nm (Figure 3a) and 120 nm (Figure 3b). The period of the fringe pattern was replicated with great fidelity by the undulating topography of the polymer films. The difference in height between exposed and unexposed regions for both cases was less than 15 nm ($^1/_2L_o$). We believe the topography depicted in Figure 3a,b accurately describes the sample surface and is not

corrupted by convolution effects in the AFM measurements because identical images were obtained using both oxide-sharpened silicon nitride tips (tip radii = 5–40 nm) and carbon nanotips (tip radii < 5 nm). To investigate the decrease in height difference with decreasing pattern dimensions, we configured the EUV interferometer to produce Fresnel diffraction fringes. As shown in Figure 4, the difference in height between adjacent regions, $\Delta h$, decreased from 15 to 3–4 nm, as $L_s$ decreased from ~1410 nm (~$47L_o$) to 240 nm ($4L_o$, $L_o$ = 30 nm). A plot of $\Delta h$ as a function of $L_s$ is shown in Figure 5. Note that $\Delta h$ = 12 nm on the film shown in Figure 4 when $L_s$ = 1000 nm, and $\Delta h$ = 15 nm on the film shown in Figure 2 where $L_s$ = 900 nm. This discrepancy cannot be explained but may be due to differences in film thickness between the two samples or to the asymmetry of the patterned features in Figure 4.

The internal lamellar structure of the film shown in Figure 4 is unknown. For $L_s$ > 1400 nm with $\Delta h = ^1/_2L_o$, it is a good assumption that adjacent regions exhibit symmetric wetting and asymmetric wetting and that $+^1/_2$ and $-^1/_2$ dislocations exist at the boundaries. We have previously reported this type of behavior for thin films of P(S-*b*-MMA) on SA films of OTS patterned with proximity X-ray lithography.[33–35] Imaging the topography of the films with AFM, in fact, turns out to be a convenient technique to image the underlying pattern of the SA films.[34] Pereira et al. have used a phenomenological model to investigate numerically the morphology of thin films of diblock copolymers on substrates patterned with alternating stripes wet by the different blocks of the copolymer where $L_s \gg L_o$.[36] It is unclear how to relate the theoretical calculations to the experimental observations since: (1) Pereira et al. explicity assumed that the difference in height between adjacent regions was equal to $L_o$, as opposed to the experimentally determined value of $^1/_2L_o$,[33–35] and (2) the topography of the film was modeled as having a step function profile at the edges of the stripes, as opposed to the more sinusoidal-like profile observed experimentally. We also note that the model of Pereira et al. predicts that the lateral distance, $L_{kink}$, over which kinks in the lamellar structure accommodate the +1 dislocation at a pattern
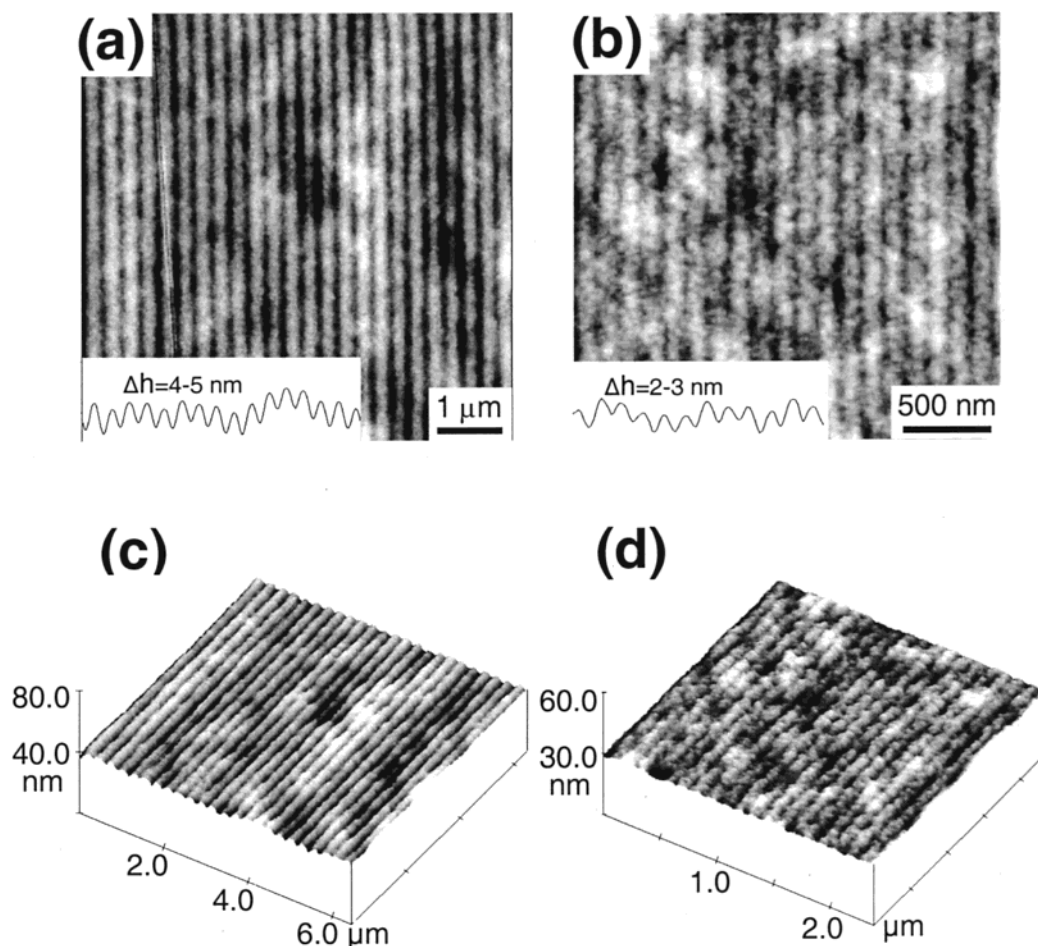
**Figure 3.** AFM images of the surface of P(S-*b*-MMA) ($L_o$ = 30 nm) film after deposition and annealing on chemically patterned surfaces with periods of (a) 240 nm and (b) 120 nm. The initial film thickness was ~$2.2L_o$ (66 ± 2 nm). The difference in height between adjacent regions was (a) 4−5 nm and (b) 2−3 nm. Three-dimensional AFM images of (a) and (b) are shown in (c) and (d), respectively.

boundary with $\Delta h = L_o$ is of order $L_o$. Data presented by Liu et al. showed $L_{kink}$ to be of order several hundered nanometers at the edge of an island with a step height of $L_o$.[37] Our data for $+^1/_2$ dislocations also indicates $L_{kink}$ to be of order several hundred nanometers.

As $L_s$ decreased below 1400 nm, $\Delta h$ decreased below $^1/_2L_o$. A number of morphologies may be consistent with this experimental observation. Two intuitive possibilities include the following: (1) Parallel lamellae with alternating symmetric wetting and asymmetric wetting where the surface topography is flattened due to surface tension forces and the lamellae are pinched ($L \neq L_o$) at the edges of the pattern. This behavior is similar to that reported by Liu et al. in which the surface profile of the edge of an island ($\Delta h = L_o$) was flattened and resulted in pinching of the lamellar domains near the −1 dislocation.[37] (2) Perpendicular lamellae or disordered lamellae are present at the edge of the pattern or throughout regions of the film. This behavior is similar to that reported by Carvalho et al.,[38] Liu et al.,[37] and Heier et al.[39] where a reorientation of lamellae was observed at the edge of islands ($\Delta h = L_o$) or similar to that reported by Heier et al. where islands over regions of perpendicular lamellae had step heights < $L_o$.[40,41] We believe the former description is more likely because we have not observed perpendicular lamellae at the pattern boundary or within the fringe pattern on our samples using either plane-view TEM or AFM.

As the period of the fringes with which the OTS was exposed approached the bulk lamellar period of the block copolymer, a different behavior was observed. Figure 6 shows an AFM phase image of P(S-*b*-MMA) film after it was annealed on an OTS surface that had been exposed using the EUV interferometer configured to produce ~60 nm fringe periods. The initial film thickness was ~60 nm ($L_o$). AFM images of the topography of the polymer films revealed that surface roughness was on the order of 1 nm, but no pattern in the roughness was observed. In phase images, however, a pattern was observed on the patterned region that matched the fringe period of the exposure. On the nonpatterned unexposed and exposed regions of the samples, there was no evidence of alignment of the features in the phase image. Figure 6 is a representative image of the film morphology that was characteristic along the entire 5 mm length of the patterned regions and that was characteristic of a number of different exposure fields. The contrast in the phase image was due to differences in chemical composition between the blocks of copolymer.[13] The PS block appears darker than the PMMA block.[11e] (Note: there was no contrast in phase images of the surfaces of the polymer films depicted in Figures 2−4.) A block copolymer film processed in exactly the same manner as the film shown in Figure 6 was prepared for TEM analysis. Figure 7 shows the in-plane-view image of the film. The PS block appears darker than the PMMA block due to staining
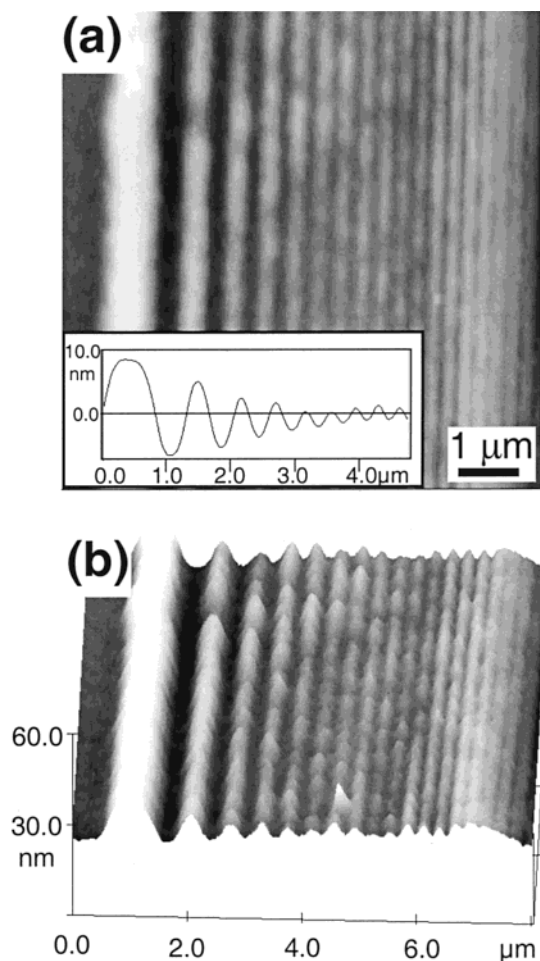
**(a)**



**(b)**

**Figure 4.** AFM images of the surface of a P(S-*b*-MMA) ($L_o =$ 30 nm) film after deposition and annealing on a surface chemically patterned with a Fresnel diffraction pattern. The period of the surface pattern decreased from ~1410 to 240 nm from left to right in the images. The initial film thickness was ~$2.2L_o$ ($66 \pm 2$ nm). (a) AFM image with cross sectional data, showing the difference in height between adjacent regions decreased from ~15 nm ($^1/_2L_o$) to 4–5 nm as $L_s$ decreased from ~1410 to 240 nm. (b) Three-dimensional AFM image of the topography of the polymer film.
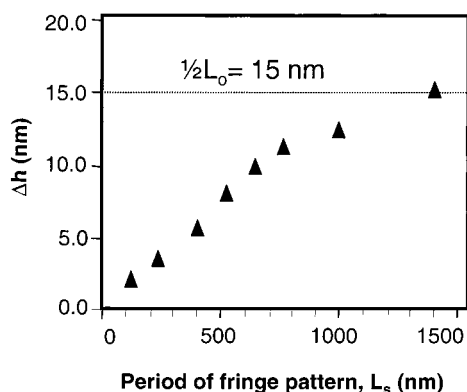


**Figure 5.** Plot of $\Delta h$ versus fringe period for the polymer film shown in Figure 4. For fringe periods greater than 1400 nm, $\Delta h$ equaled 15 nm ($^1/_2L_o$). As the fringe period decreased, $\Delta h$ decreased to a minimum of ~3 nm for a fringe period of 240 nm.

with $RuO_4$. The phase image and the TEM image provide conclusive evidence that the lamellae are oriented perpendicular to the substrate and are aligned with the underlying pattern in chemical functionality over macroscopic dimensions.
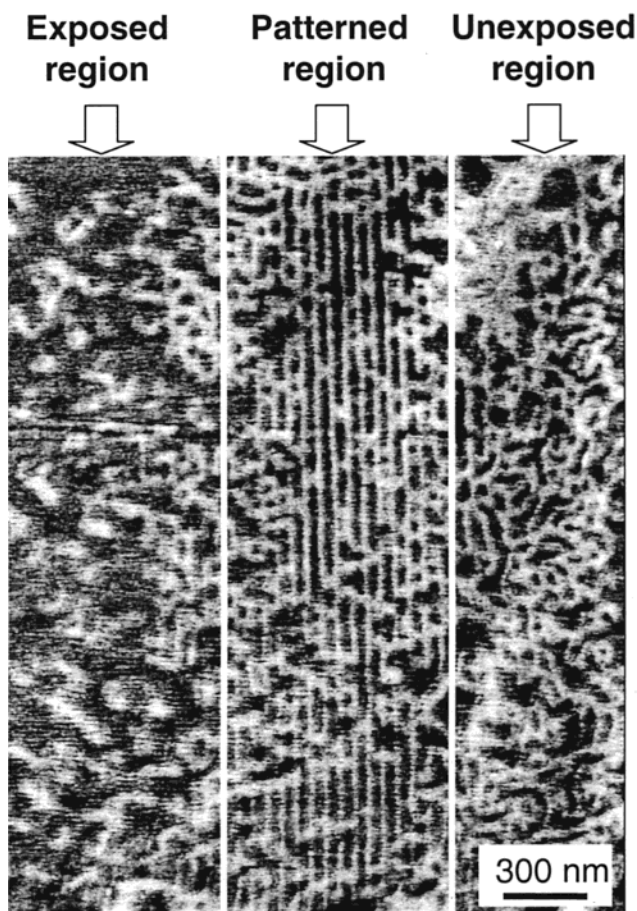
**Exposed region** **Patterned region** **Unexposed region**



**Figure 6.** Tapping-mode AFM phase image of the surface of a P(S-*b*-MMA) ($L_o = 66$ nm) film after deposition and annealing on a chemically patterned surface with a period of ~$L_o$. The initial film thickness was ~$L_o$ (60 nm). The lamellae were oriented perpendicular to the plane of the film and amplified the surface pattern. The contrast in the phase image was due to differences in chemical composition between the blocks of copolymer with the PS block appearing darker than the PMMA block.

It is unknown whether defects in the perpendicular lamellar structures shown in Figures 6 and 7 were present only on the surface or extended through out the entire thickness of the film. The defects were unlikely to be due to defects in the patterning of the OTS because imperfections were rarely observed in patterned resist. One reason for the defects may be that $L_o$ was slightly larger than $L_s$. We measured $L_o$ to be $67.8 \pm 1.6$ nm from the TEM images in Figure 7, $65 \pm 2$ nm from the AFM phase image in Figure 6, and $66 \pm 1.3$ nm from the step heights of holes on a thin film on a homogeneous surface using AFM. We measured $L_s$ from patterned photoresist to be $63 \pm 1$ nm. The ratio of $L_o$ to $L_s$, therefore, could have ranged from 0.98 to 1.12. Rockford et al. have shown that defects are more likely as $L_o$ and $L_s$ become more incommensurate.[13] It is also possible that the lamellae are perfectly registered with the chemical pattern at the substrate interface and that the defects are due to segregation of PS at the surface.[15,19] PS preferentially segregates to the free surface because PS has a lower surface tension than that of PMMA. We have observed similar defects for films with lamellae oriented perpendicular to the substrate annealed on neutral wetting substrates.[27] By etching and imaging the films on neutral substrates at different depths, the defects were shown to be only at the free
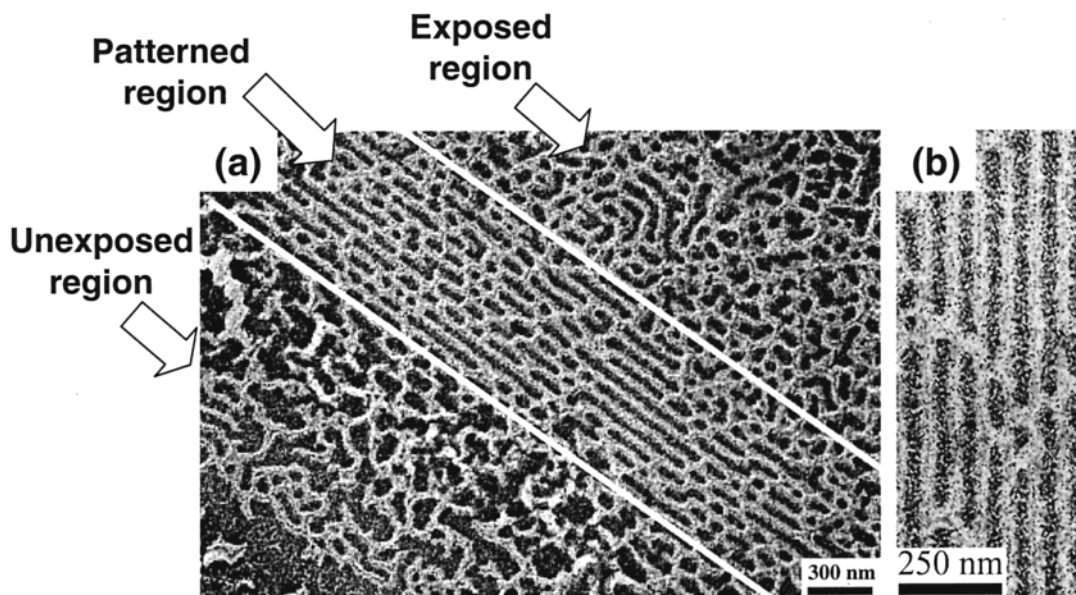
**Figure 7.** (a) In-plane-view TEM image of a P(S-*b*-MMA) ($L_o$ = 66 nm) film after deposition and annealing on a chemically patterned surface with a period of $L_o$. The initial film thickness was ~$L_o$ (60 nm). The PS block appears darker than the PMMA block due to staining with $RuO_4$. The lamellae were oriented perpendicular to the plane of the film and amplified the surface pattern. (b) In-plane-view TEM image of a second region of the polymer film shown in (a).

surface. This type of analysis was not possible in this study because the total film thickness was only 60 nm.

Orientation of lamellae perpendicular to the substrate and registration of the domains with an underlying pattern in wetting behavior is in agreement with simulation, theory, and experimental work in the literature. Wang et al. investigated the morphology of symmetric block copolymer films confined between patterned and homogeneous surfaces using Monte Carlo simulations[15] and used this information to construct phase diagrams with a simple phenomenological theory.[19] In agreement with our experiments, perpendicular lamellae aligned with the surface pattern were predicted when the surface pattern period was comparable to the bulk lamellar period of the block copolymer and the upper boundary condition for the film is a neutral or weakly preferential surface.

The experiments presented here build on previous work by Rockford et al.[13] They demonstrated orientation of lamella of P(S-*b*-MMA) perpendicular to the substrate and aligned with a surface pattern consisting of alternating gold and $SiO_x$ stripes when the surface pattern period was commensurate with the bulk lamellar period of the block copolymer. The substrates were prepared by annealing miscut silicon to produce topographic patterns of bunched steps and terraces ($\Delta h \approx 10$ nm). A striped surface was created by obliquely depositing gold and taking advantage of a shadowing effect. Advantages of producing surface patterns using advanced lithography instead of miscut silicon include (1) the surface patterns are purely chemical with no topography according to our AFM characterization, (2) perfection in the surface patterns extends over macroscopic dimensions, potentially millimeters, (3) the dimensions of the patterns are easily manipulated, and (4) patterns other than stripes are readily obtainable. The use of advanced lithography also enables registration of the pattern with features of the underlying substrate, and the process is compatible with standard microelectronic processing techniques. The use of substrates patterned with advanced lithography in conjuction with self-assembly from the melt may allow block

copolymers to be used to fabricate addressable arrays over large areas at the scale of 10 nm.

Another major difference between the experiments of Rockford et al. and those presented above is the process of depositing the block copolymer films. Rockford et al. put a drop of a dilute solution of P(S-*b*-MMA) in toluene on their substrates and slowly evaporated the solvent. We do not know whether the reported morphologies of the films are representative of the entire polymer film or are representative of the morphology near the edge of the drop or whether the solvent-annealed films are uniform in thickness. The block copolymer films of uniform initial thickness in this study were deposited via spin-coating over large areas that included both patterned and unpatterned areas. The morphology of the film self-assembled in the melt during annealing at temperatures above the glass transition temperature of both blocks. The method of Rockford et al. may be advantageous in terms of producing fewer defects. The solvent imparts greater mobility to the polymer, and the nonpreferential nature of the solvent may effectively create a neutral boundary condition at the free surface. The advantage of thermal annealing is ease and reproducibility of processing.

## Conclusions

We have developed a technique to control the orientation of lamellar domains in supported thin films of P(S-*b*-MMA). Advanced lithographic techniques were used to chemically pattern an imaging layer to guide the self-assembly of diblock copolymer films. Experimental results showed that if the period of the striped pattern in wetting behavior on the surface was greater than $L_o$, the lamellae structure of P(S-*b*-MMA) films was orientated parallel to substrate and exhibited topography that replicated the underlying pattern of the surface. The difference in height between adjacent regions had a maximum value of $^1/_2L_o$ and decreased as $L_s$ approached $L_o$. If the period of the surface patterns was commensurate with $L_o$, the lamellae structure was oriented perpendicular to the substrate and amplified

the pattern of the imaging layer. Guided self-assembly of lamellae in block copolymer films was observed over macroscopic dimensions.

## References and Notes

(1) Harrison, C.; Park, M.; Chaikin, P. M.; Register, R. A.; Adamson, D. H. *J. Vac. Sci. Technol. B* **1998**, *16*, 544.
(2) Park, M.; Harrison, C.; Chaikin, P. M.; Register, R. A.; Adamson, D. H. *Science* **1997**, *276*, 1401.
(3) Bates, F. S.; Fredrickson, G. H. *Annu. Rev. Chem.* **1990**, *41*, 525.
(4) Bates, F. S. *Science* **1991**, *251*, 898.
(5) Harrison, C.; Chaikin, P. M.; Huse, D. A.; Register, R. A.; Adamson, D. H.; Daniel, A.; Huang, E.; Mansky, P.; Russell, T. P.; Hawker, C. J.; Egolf, D. A.; Melnikov, I. V.; Bodenschatz, E. *Macromolecules* **2000**, *33*, 857.
(6) Coulon, G.; Russell, T. P.; Deline, V. R.; Green, P. F. *Macromolecules* **1989**, *22*, 2581.
(7) Coulon, G.; Collin, B.; Ausserre, D.; Chatenay, D.; Russell, T. P. *J. Phys. (Paris)* **1990**, *51*, 2801.
(8) Russell, T. P.; Coulon, G.; Deline, V. R.; Miller, D. C. *Macromolecules* **1989**, *22*, 4600.
(9) Anastasiadis, S. H.; Russell, T. P.; Satija, S. K.; Majkrzak, C. F. *Phys. Rev. Lett.* **1989**, *62*, 1852.
(10) (a) Morkved, T. L.; Lu, M.; Urbas, A. M.; Ehrichs, E. E.; Jaeger, H. M.; Mansky, P.; Russell, T. P. *Science* **1996**, *273*, 931. (b) Mansky, P.; DeRouchey, J.; Russell, T. P.; Mays, J.; Pitsikalis, M.; Morkved, T.; Jaeger, H. *Macromolecules* **1998**, *31*, 4399.
(11) (a) Mansky, P.; Liu, Y.; Huang, E.; Russell, T. P.; Hawker, C. *Science* **1997**, *275*, 1458. (b) Mansky, P.; Russell, T. P.; Hawker, C. J.; Pitsikalis, M.; Mays, J. *Macromolecules* **1997**, *30*, 6810. (c) Huang, E.; Russell, T. P.; Harrison, C.; Chaikin, P. M.; Register, R. A.; Hawker, C. J.; Mays, J. *Macromolecules* **1998**, *31*, 7641. (d) Huang, E.; Rockford, L.; Russell, T. P.; Hawker, C. J. *Nature* **1998**, *395*, 757. (e) Thurn-Albrecht, T.; Steiner, R.; DeRouchey, J.; Stafford, C. M.; Huang, E.; Bal, M.; Tuominen, M.; Hawker, C. J.; Russell, T. P. *Adv. Mater.* **2000**, *12*, 757. (f) Thurn-Albrecht, T.; DeRouchey, J.; Russell, T. P.; Jaeger, H. M. *Macromolecules* **2000**, *33*, 3250.
(12) Fasolka, M. J.; Harris, D. J.; Mayes, A. M.; Yoon, M.; Mochrie, S. G. J. *Phys. Rev. Lett.* **1997**, *79*, 3018.
(13) Rockford, L.; Liu, Y.; Mansky, P.; Russell, T. P.; Yoon, M.; Mochrie, S. G. J. *Phys. Rev. Lett.* **1999**, *82*, 2602.
(14) Segalman, R. A.; Yokoyama, H.; Kramer, E. J. Presented at American Physical Society Meeting, Minneapolis, March 2000.
(15) Wang, Q.; Yan, Q. L.; Nealey, P. F.; de Pablo, J. J. *Macromolecules* **2000**, *33*, 4512.
(16) Semenov, A. N. *Sov. Phys. JETP* **1985**, *61*, 733.
(17) Wang, Z.-G. *J. Chem. Phys.* **1994**, *100*, 2298.
(18) Ohta, T.; Kawasaki, K. *Macromolecules* **1986**, *19*, 2621.
(19) Wang, Q.; Nath, S. K.; Graham, M. D.; Nealey, P. F.; de Pablo, J. J. *J. Chem. Phys.* **2000**, *112*, 9996.
(20) Chakrabarti, A.; Chen, H. *J. Polym. Sci., Part B* **1998**, *36*, 3127.
(21) Chen, H.; Chakrabarti, A. *J. Chem. Phys.* **1998**, *108*, 6897.
(22) Petera, D.; Muthukumar, M. *J. Chem. Phys.* **1997**, *107*, 9640.
(23) Petera, D.; Muthukumar, M. *J. Chem. Phys.* **1998**, *109*, 5101.
(24) Pereira, G. G.; Williams, D. R. M. *Macromolecules* **1999**, *32*, 758.
(25) Halperin, A.; Sommer, J. U.; Daoud, M. *Europhys. Lett.* **1995**, *29*, 297.
(26) Kim, T. K.; Yang, X. M.; Peters, R. D.; Sohn, B. H.; Nealey, P. F. *J. Phys. Chem. B* **2000**, *104*, 7403.
(27) Peters, R. D.; Yang, X. M.; Kim, T. K.; Sohn, B. H.; Nealey, P. F. *Langmuir* **2000**, *16*, 4625.
(28) Peters, R. D.; Yang, X. M.; Kim, T. K.; Nealey, P. F. *Langmuir* **2000**, *16*, 9620.
(29) Solak, H. H.; He, D.; Li, W.; Singh-Gasson, S.; Cerrina, F.; Sohn, B. H.; Yang, X. M.; Nealey, P. *Appl. Phys. Lett.* **1999**, *75*, 2328.
(30) Solak, H. H.; He, D.; Li, W.; Cerrina, F. *J. Vac. Sci. Technol. B* **1999**, *17*, 3052.
(31) Laibinis, P. E.; Graham, R. L.; Biebuyck, H. A.; Whitesides, G. M. *Science* **1991**, *254*, 981.
(32) Graham, R. L.; Bain, C. D.; Biebuyck, H. A.; Laibinis, P. E.; Whitesides, G. M. *J. Phys. Chem.* **1993**, *97*, 9456.
(33) Yang, X. M.; Peters, R. D.; Kim, T. K.; Nealey, P. F. *J. Vac. Sci. Technol. B* **1999**, *17*, 3203.
(34) Yang, X. M.; Peters, R. D.; Kim, T. K.; Nealey, P. F.; Brandow, S. L.; Chen, M.-S.; Shirey, L. M.; Dressick, W. J. *Langmuir*, in press.
(35) Peters, R. D.; Yang, X. M.; Kim, T. K.; Nealey, P. F. Presented at American Physical Society Meeting, Atlanta, March 1999.
(36) Pereira, G. G.; Williams, D. R. M.; Chakrabarti, A. *J. Chem. Phys.* **2000**, *112*, 10011.
(37) Liu, Y.; Rafailovich, M. H.; Sokolov, J.; Schwarz, S. A.; Bahal, S. *Macromolecules* **1996**, *29*, 899.
(38) Carvalho, B. L.; Thomas, E. L. *Phys. Rev. Lett.* **1994**, *73*, 3321.
(39) Heier, J.; Kramer, E. J.; Groenewold, J.; Fredrickson, G. H. *Macromolecules* **2000**, *33*, 6060.
(40) Heier, J.; Genzer, J.; Kramer, E. J.; Bates, F. S.; Walheim, S.; Krausch, G. *J. Chem. Phys* **1999**, *111*, 11101.
(41) Heier, J.; Sivaniah, E.; Kramer, E. J. *Macromolecules* **1999**, *32*, 9007.